Biochemical and Biophysical Research Communications 485 (2017) 584–590

Contents lists available at ScienceDirect

Biochemical and Biophysical Research Communications

journal homepage: www.elsevier.com/locate/ybbrc

Crystal structure of the PDZ domain of mouse Dishevelled 1 and its interaction with CXXC5

Inhwan Lee [a], Sooho Choi [a], Ji-Hye Yun [a], Seol hwa Seo [b, c], Sehee Choi [b, c], Kang-Yell Choi [b, c], Weontae Lee [a, *]

[a] Department of Biochemistry, College of Life Science and Biotechnology, Yonsei University, Seoul 120-740, South Korea
[b] Department of Biotechnology, College of Life Science and Biotechnology, Yonsei University, Seoul 120-749, South Korea
[c] Translational Research Center for Protein Function Control, Yonsei University, Seoul 120-749, South Korea

ARTICLE INFO

Article history:
Received 26 November 2016
Accepted 3 December 2016
Available online 6 December 2016

Keywords:
Dvl-1
PDZ domain
CXXC5
Wnt signaling
X-ray crystallography

ABSTRACT

Dishevelled (Dvl) plays a crucial role in Wnt signaling by interacting with membrane-bound receptors and downstream molecules through its PDZ domain. CXXC5 is one of the key molecules that interacts with Dvl and negatively regulates the Wnt/β-catenin pathway in osteoblast differentiation. Recently, the Dvl-CXXC5 interaction has been identified as an excellent target for osteoporosis treatment. Therefore, it is desirable to have detailed structural information for the Dvl-CXXC5 interaction. Although solution structures of the Dvl1 PDZ domain have been reported, a high-resolution crystal structure would provide detailed sidechain information that is essential for drug development. Here, we determined the first crystal structure of the Dvl-1 PDZ domain at a resolution of 1.76 Å, and compared it with its previously reported solution structure. The Dvl1 PDZ domain crystal belonged to the space group H32 with unit-cell parameters a = b = 72.837, c = 120.616, α = β = 90.00, γ = 120.00. The crystal structure of Dvl1 PDZ shared its topology with the previously reported structure determined by nuclear magnetic resonance (NMR); however, the crystal structure was quite different from the solution structure in both the secondary structural region and the ligand-binding pocket. Molecular modeling based on NMR and X-ray crystallographic data yielded detailed information about the Dvl1/CXXC5 interaction, which will be useful for designing inhibitors.

1. Introduction

Wnt signaling is a signal transduction pathway that regulates development and tissue homeostasis in animals [1–5]. The Wnt pathway can be characterized into three categories, canonical, non-canonical (planar cell polarity), and non-canonical Wnt/calcium pathways [6]. The Dishevelled (Dvl) protein plays important roles in both canonical and non-canonical Wnt signaling pathways by associating with a variety of signaling molecules and receptors [7,8]. Dvl is composed of three conserved domains, namely an N-terminal DIX domain involved in Dvl polymerization, as well as a central PDZ domain and a C-terminal DEP domain, which are both essential for the binding of Dvl to other signal transduction molecules. Among these domains, the PDZ domain plays a crucial role in binding to the membrane-bound receptor Frizzled and to other signal transduction molecules in the cytoplasm. The ability of the Dvl PDZ domain to distinguish between suitable binding partners makes it an interesting therapeutic target for Wnt-signaling-associated diseases such as cancer and osteoporosis [9–12]. Recently, Dvl has been shown to be co-localized with CXXC finger protein 5 (CXXC5) in the cytoplasm by co-immunoprecipitation experiments [13]. More recently, we showed that the interaction of Dvl with CXXC5 regulates bone formation in pre-osteoblasts and that CXXC5 inhibits osteoblast differentiation by binding to Dvl [14]. CXXC5 is a member of a small family of proteins that contain CXXC-type zinc-finger domains, and it is localized in the cytosol of neural stem cells and interacts with Dvl to inhibit the Wnt/β-catenin pathway. Three Dvl homologues have been identified in humans and mice (Dvl1, 2, and 3). A solution structure of Dvl1 PDZ has previously been determined by nuclear magnetic resonance (NMR) spectroscopy [10,15]. Here, we report the first high-

* Corresponding author. Department of Biochemistry, College of Life Science and Biotechnology, Yonsei University, 134 Shinchon-Dong, Seodaemoon-Gu, Seoul 120-749, South Korea.
E-mail address: wtlee@yonsei.ac.kr (W. Lee).

http://dx.doi.org/10.1016/j.bbrc.2016.12.023
0006-291X/

resolution crystal structure of the mouse Dvl1 PDZ domain and propose a model for the interaction between the Dvl1 PDZ domain and the binding region of CXXC5 based on the crystal structure.

2. Materials and methods

2.1. Cloning, over-expression, and purification of the Dvl1 PDZ

The Dvl1 PDZ domain from mouse Dvl1 was amplified by polymerase chain reaction. The amplified cDNA fragments were subcloned into the modified expression vector pET21b (Novagen, Madison, WI) with a fused hexa-histidine tag and a *Tobacco etch virus* (TEV) protease recognition site at the N-terminus. The resulting plasmid was transformed into *Escherichia coli* (strain BL21 DE3). Dvl1 PDZ domain expressing cells were grown in Luria–Bertani media at 37 °C until they reached an OD_{600} of 0.7, at which time 0.5 mM isopropyl β-D-thiogalactopyranoside (IPTG) was added and the cells were cultured for a further 15 h at 18 °C. Cells were harvested by centrifugation and stored at −80 °C. Harvested cells were disrupted by sonication in lysis buffer [25 mM sodium phosphate, 100 mM NaCl, 5 mM β-mercaptoethanol, and protease inhibitor cocktail (Sigma-Aldrich, St. Louis, MO), pH 7.8] The $(His)_6$-tagged fusion protein was purified by immobilized metal affinity chromatography on a Ni-NTA column (Amersham Pharmacia Biotech, Little Chalfont, UK) and the $(His)_6$ tag was cleaved by incubation with TEV protease for 12 h at 25 °C. The purified Dvl1 PDZ was then further purified by size exclusion chromatography using a HiLoad™ Superdex™ 75 preparative grade column (Amersham Pharmacia Biotech). Final buffer [10 mM HEPES (pH 7.5), 100 mM NaCl, and 2 mM dithiothreitol] was used as a mobile phase during the chromatography and protein eluted with this buffer was used for crystallization. Isotope-labeled proteins for NMR experiments were over expressed in M9 minimal media overnight under the 1 mM IPTG, 25 °C condition using U-^{13}C-glucose and/or $^{15}NH_4Cl$ as sources of carbon and nitrogen, respectively.

2.2. Crystallization

The purified Dvl1 PDZ in the final buffer was concentrated to 5 mg/mL. Crystallization screening was carried out with a mosquito® crystallization robot (TTP Labtech, Melbourn, UK) using commercial screen kits from Hampton Research (Aliso Viejo, CA) and Rigaku (Tokyo, Japan). The initial crystal was observed in 0.5 M ammonium sulfate, 0.1 M sodium citrate tribasic dihydrate pH 5.6, and 1.0 M lithium sulfate monohydrate. By simply increasing the volume of the crystallization drop, we could obtain a crystal of a suitable size for diffraction. Equal volumes of protein solution and mother liquor (2 μL + 2 μL) were mixed in a 24-well sitting drop plate and crystals were grown at 15 °C.

2.3. Data collection and processing

Crystals soaked in crystallization solution with an additional 17% (*v*/*v*) ethylene glycol added for cryo-protection were flash-cooled to 100 K in liquid nitrogen. Diffraction data were collected using an ADSC Q270 CCD detector on the 7A beamline at the Pohang Accelerator Laboratory (PAL), Pohang, Korea. The distance from detector to crystal was 210 mm and a total of 360 images were collected with oscillation widths of 1°, exposing the crystal to the beam for 1 s per image. Data were integrated and scaled using the HKL2000 package [16]. The diffraction data were collected at a maximum resolution of 1.76 Å. Data collection statistics are summarized in Table 1.

Table 1
Data collection and refinement statistics.

	Dvl1 PDZ
Data collection	
Space group	H32
Cell dimensions	
a, b, c (Å)	72.837 72.837 120.616
α20.616 (ns)	90.00 90.00 120.00
Resolution (Å)	30.00–1.76 (2.07–2.00)[a]
R_{sym} or R_{merge}	0.072 (0.155)
$I/\sigma(I)$	42.49 (3.05)
Completeness (%)	99.2 (92.5)
Redundancy	8.1 (4.8)
Refinement	
Resolution	30.00–1.76 (2.006)
No. reflections	1187
R_{work}/R_{free}	0.1778/0.2254
N.o atoms	
Protein	718
Water	0
Root mean square deviations	
Bond lengths	0.019
Bond angles	1.944

[a] Values in parentheses are for highest-resolution shell.

2.4. Structure determination and refinement

The phase problem was solved by molecular replacement using the structure of the Dvl2 PDZ domain (PDB: 2REY) as a search model with the Phenix software suite [17]. Model re-building and refinement was performed iteratively with Coot [18] and Molrep in the CCP4 suite [19], respectively. Structural statistics after refinement are summarized in Table 1.

2.5. Molecular docking

A model of the molecular docking between Dvl1 PDZ and the binding region of CXXC5 (Dvl-binding motif [DBM] peptide) complex was generated using the FlexPepDock server implemented within the Rosetta framework [20,21]. The high-resolution crystal structure of Dvl1 PDZ determined in this study was prepared and a flexible 13-amino-acid DBM peptide was used as an input model to dock into the conventional Dvl1 PDZ peptide binding site. The model with the highest score based on the Rosetta generic full-atom energy function was selected [22]. The predicted structure of the complex was visualized and figures were created using the PyMOL program (DeLano Scientific LLC, San Carlos, CA).

2.6. NMR spectroscopy

NMR experiments were performed at 298 K on a Bruker 600 MHZ spectrometer equipped with a z-shielded gradient triple resonance cryoprobe. Sequential resonance assignment was executed by experiments of $^{1}H–^{15}N$ HSQC [23], 3D HNCACB, CBCACONH, HBHACONH, and HNCA [24]. To investigate the dynamic properties of the Dvl1 PDZ domain upon CXXC5 binding, heteronuclear $^{1}H,^{15}N$ nuclear Overhauser effects (XNOE) (ref) were measured with and without DBM peptide. Unsaturated and saturated XNOE spectra were acquired by interleaving pulse sequences and were separately processed using the XWINNMR program. The XNOE data were performed for $t_2 \times t_1$ dimensions with a 5-s recycle delay.

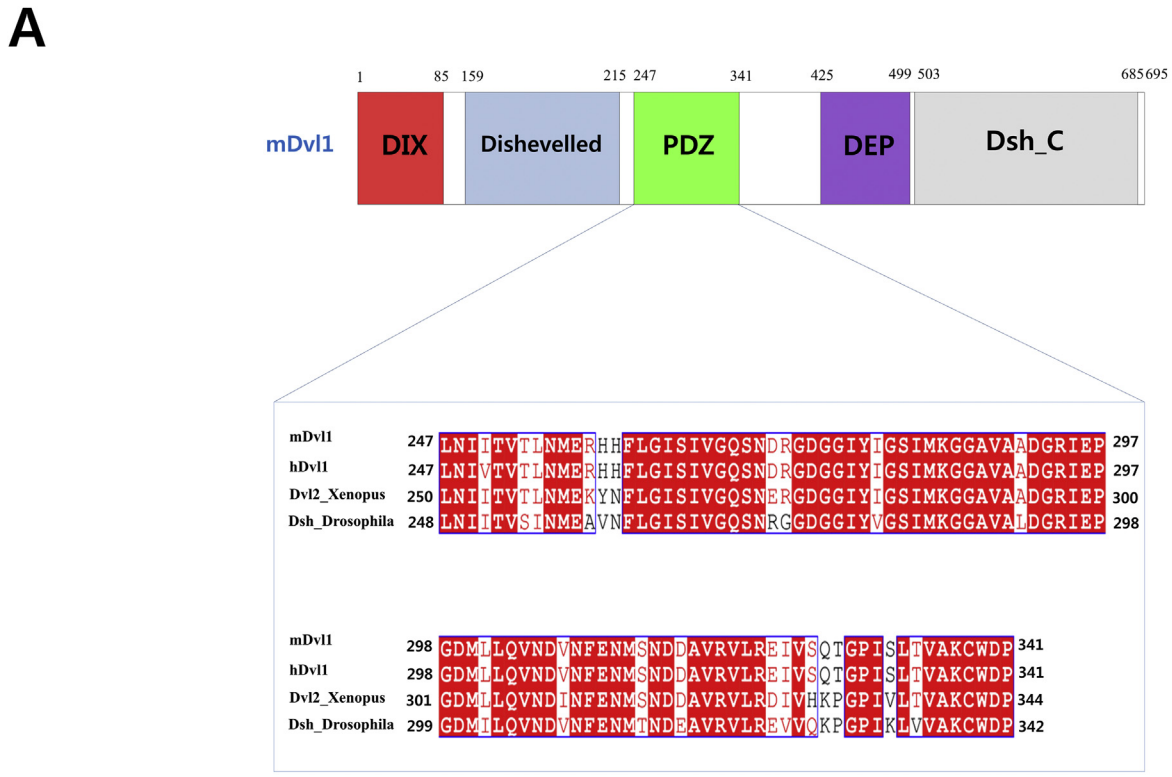

Fig. 1. Domain organization of mouse Dvl1 (mDvl1) and multiple sequence alignment of the Dvl1 PDZ domains. (A) The sequence of the PDZ domain located at the center of mDvl1 was aligned with the sequences of the PDZ domains from the human, *Xenopus*, and *Drosophila* Dvl homologues (aligned using the T-Coffee server and drawn using ESPript 3.0). (B) The overall crystal structure of the mDvl1 PDZ is presented as a cartoon representation. The conventional peptide-binding region of the PDZ domain is depicted in green color. The front view of the peptide-binding region is shown on the left. The top view of the region is shown on the right. (For interpretation of the references to colour in this figure legend, the reader is referred to the web version of this article.)

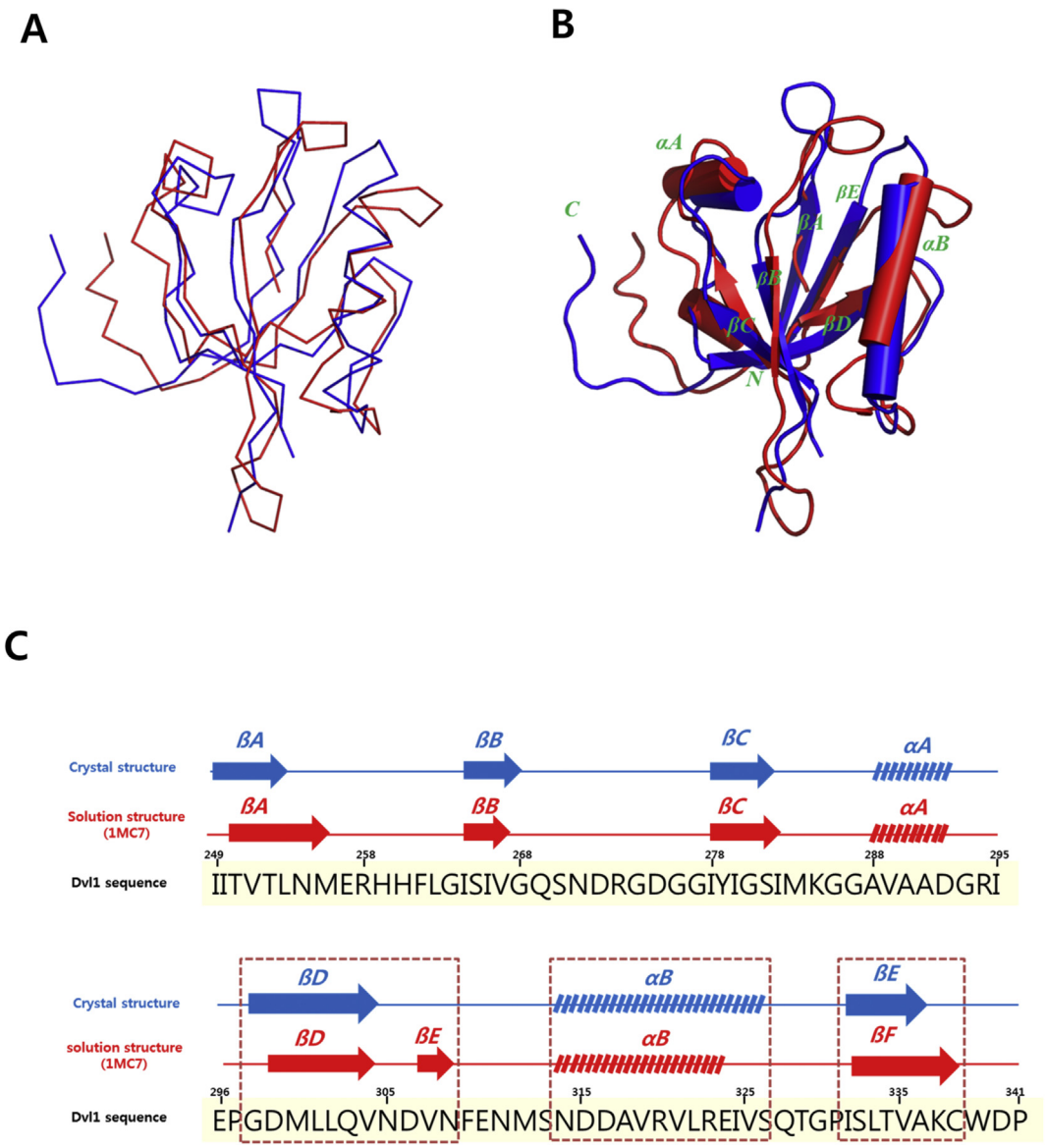

Fig. 2. Structural comparison of the two mDvl1 PDZ domains. (A and B) The solution structure (PDB: 1MC7) and the crystal structure of mDvl1 were superimposed and shown as ribbon (A) and cylinder (B) models. Solution structures are colored red and crystal structures are colored blue. Secondary structures are labeled on the crystal structure. (C) The lengths of the secondary structural elements of the Dvl1 PDZ crystal structure (blue) and solution structure (red) are compared. Regions with large differences between the two structures are shown in red dotted boxes. (For interpretation of the references to colour in this figure legend, the reader is referred to the web version of this article.)

3. Results and discussion

3.1. Crystal structure of Dvl1 PDZ domain

Dvl1 is composed of five conserved domains: DIX, Dishevelled domain, PDZ, DEP, and C-terminal domain (Fig. 1A). Among the five domains of Dvl1, the PDZ domain plays an important role in protein interaction and lies at the center of the Dvl1 protein, comprising residues 247–341. The PDZ domain is well conserved among the Dvl proteins with sequence identities of 99% (human Dvl1) and 89% (*Xenopus*). Crystals of Dvl1 PDZ were diffracted to 1.76 Å resolution at the synchrotron beamline 7A at PAL and their structure was successfully solved by the molecular replacement method using the crystal structure of the Dvl2 PDZ domain (PDB: 2REY) as a search model. The structure of the Dvl1 PDZ is an α/β fold with five anti-parallel β strands flanked by two α helices (Fig. 1B). As previously reported, αB and βB were found to form a cleft in the conventional peptide binding site [25]. Dvl PDZ folds into a compact globular structure with a diameter of about 28 Å. A loop connecting βA and βB forms a well-ordered structure that was clearly visible in the electron density map. However, residues 273–275 in the loop between βB and βC were not visible in the electron density map due to the flexibility of that region. One glycine residue at the N-terminus, which is a remnant of the fusion tag after its cleavage, and residues 26–27 in the loop region were not visible in the electron density map, but the entire C-terminal chain could be built in the clear density map. Matthew's coefficient and the solvent content calculated from CCP4i were 2.87 and 57.13%, respectively, with one molecule per asymmetric unit.

3.2. Comparison of the crystal structure with the solution structure

The crystal structure of the Dvl1 PDZ domain has the same amino acid sequence as the solution structure (PDB: 1MC7), except

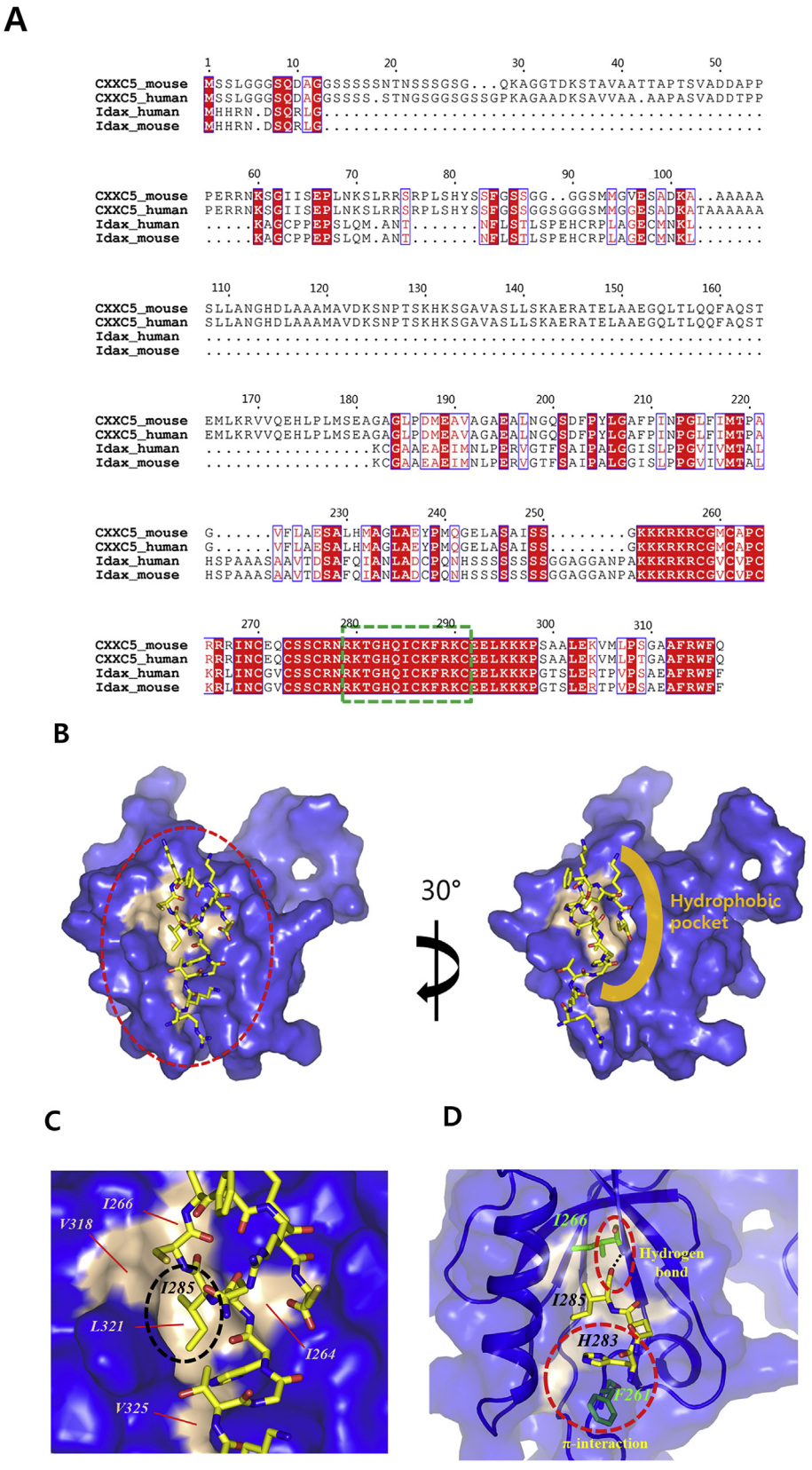

Fig. 3. The predicted docking model of the Dvl1 PDZ domain in complex with CXXC DBM. (A) Multiple sequence alignment of human and mouse Idax and CXXC5. The conserved DBM sequence is shown in a green dotted box. (B) DBM peptide docked in the conventional peptide-binding site of the Dvl1 PDZ. The DBM peptide was shown as a ball-stick model and Dvl1 PDZ is presented as a surface model colored in blue, with the hydrophobic residues comprising the binding pocket represented in a wheat color. (C) Interactions between Dvl1 PDZ and DBM peptide in zoomed view. I290 (in the black dotted circle) at the center of the DBM peptide was well docked into the hydrophobic pocket composed of I264, I266, L318, L321, and L325 in the Dvl1 PDZ. (D) A hydrogen bond between the backbones of I290 of CXXC5 and I266 in Dvl1 PDZ and the pi-interaction between H283 of CXXC5 and F261 of Dvl PDZ stabilize the CXXC5/PDZ interaction. I266 and F268 in PDZ are colored in green and the hydrogen bond and pi-interaction are enclosed in red dotted circles. (For interpretation of the references to colour in this figure legend, the reader is referred to the web version of this article.)

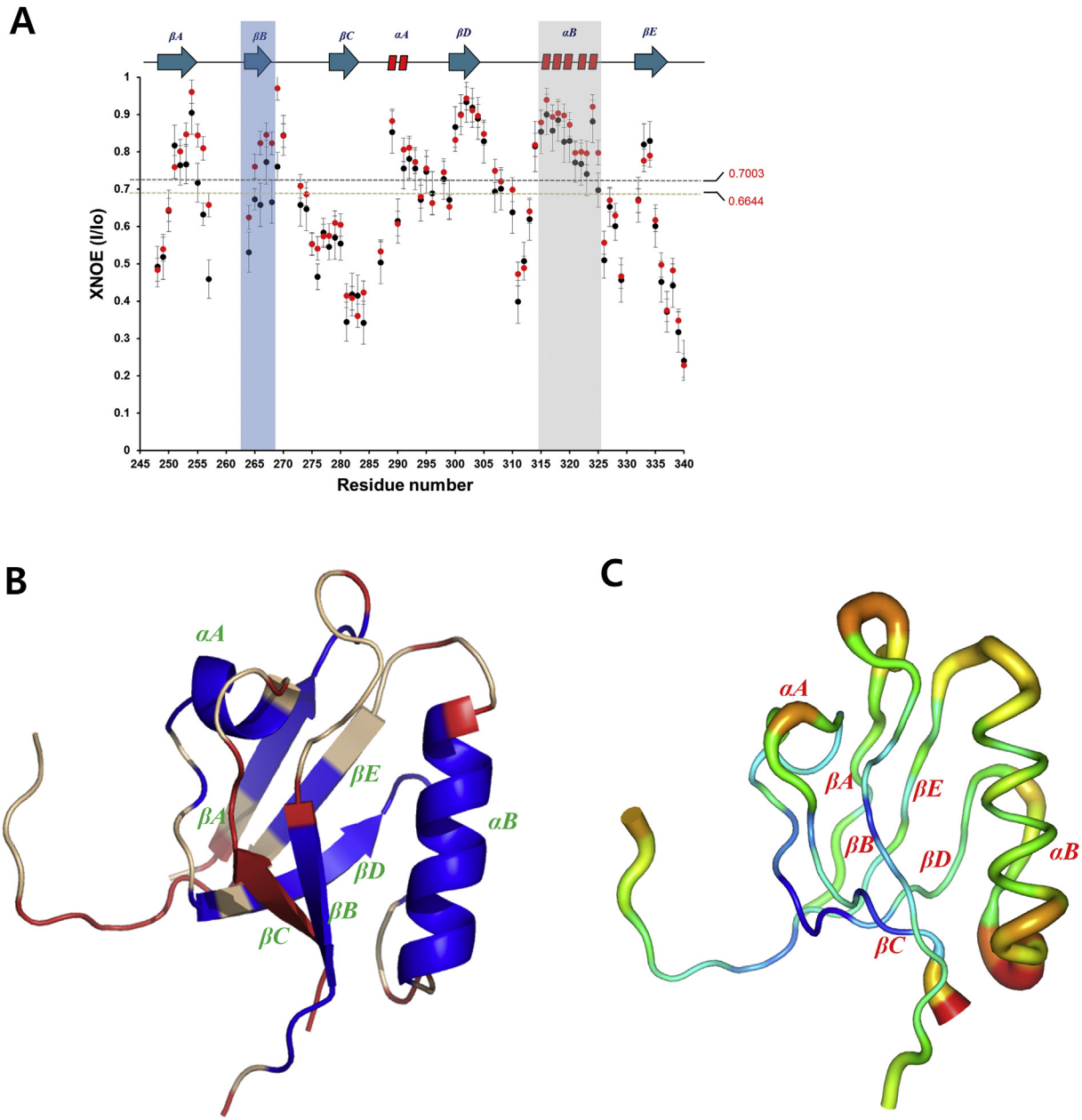

Fig. 4. Dynamics of the structure of mDvl1 PDZ. (A) Heteronuclear nuclear Overhauser effects (XNOEs) of both the free Dvl1 PDZ and its complex form with CXXC5 peptide were plotted for each residue and the corresponding secondary structures were drawn above the panel. The peptide binding sites βB and αB are shown in the blue and gray shaded boxes, respectively, and the peptide-bound state is indicated by black dots, while the peptide-free state is indicated by red dots. (B) XNOE values of the peptide-unbound state of the Dvl1 PDZ are labeled on the Dvl1 PDZ crystal structure. Residues with values higher than 0.7 are colored in blue and those with values lower than 0.6 are colored in red. Values between 0.6 and 0.7 are colored in wheat. (C) B-factor putty representation of the crystal structure of Dvl1 PDZ. Residues with high B-factors are depicted by a wider tube with a red color and low B-factors by a narrower tube with a blue color. (For interpretation of the references to colour in this figure legend, the reader is referred to the web version of this article.)

that it lacks five additional residues at the N-terminus, including one glycine remaining from the cleaved fusion tag. The crystal structure of Dvl PDZ was superimposed with that of the solution state (PDB: 1MC7), and subtle differences were identified in both secondary structures and the peptide-binding region (Fig. 2A). The overall backbone root mean square deviation on C^{α} atoms was calculated as 2.43 Å between the two structures. Notably, differences between the solution and crystal structures were observed in the conventional peptide-binding site formed by β2 and α2. The position of the C^{α} of Ile264 in β2, which is located in the peptide-binding pocket, was moved approximately 2.07 Å backward, causing β3 to be twisted in the opposite direction to the binding site. Structural differences were clearly seen from the cylindrical cartoon representation, where αB, which is involved in peptide binding, is shifted about 12.9° (Fig. 2B). A summary of the differences between the solution and crystal structures in the secondary structural regions is shown in Fig. 2C. For example, βD spans from 298G to 304V in the crystal structure, whereas it spans from 299D to 304V followed by a short additional strand (βE: 307V–308N) in the solution state (Fig. 2C). In addition, the precise spatial coordinates of a loop located between β1 and β2 fluctuated by about 9 Å, indicating that regions of the peptide-binding pocket may have dynamic conformations. A characteristic feature of PDZ domains is the plasticity of their ligand interactions, creating a versatile

interaction module in multicellular organisms [26]. This conformational flexibility in the peptide-binding pocket likely allows the ligand-binding pocket to accommodate diverse ligands, which is a general feature of PDZ domains [27].

3.3. Interaction between Dvl PDZ and CXXC5

A 13-residue peptide with the sequence RKTGHQICKFRKC in the zinc finger domain has been identified from the Idax (CXXC5) protein as a DBM peptide and the primary sequence is well conserved at the C-terminus of the CXXC5 proteins and Idax (Fig. 3A). The docking of the DBM peptide derived from CXXC5 with the crystal structure of Dvl1 PDZ was assessed using the FlexPepDock web server [20,21]. The results showed that the DBM peptide binds onto the peptide-binding pocket of the Dvl PDZ (Fig. 3B). Residues of I264, I266, V318, L321, and V325 of the Dvl PDZ formed a hydrophobic binding pocket and I285 of the DBM peptide was well accommodated onto the pocket (Fig. 3C). Especially, the backbone carbonyl oxygen of I285 of CXXC5 and the amide nitrogen of I266 of Dvl PDZ stabilize the interaction via forming a hydrogen bond (Fig. 3D).

3.4. Dynamic profile of Dvl1 PDZ

The protein dynamics of the Dvl1 PDZ in solution was measured by XNOE experiments. The average values for XNOEs were 0.6644 and 0.7003 for the peptide-free and bound states, respectively (Fig. 4A). Data of XNOE experiments indicate that the global structure of the Dvl PDZ becomes rigid upon peptide binding. Especially, XNOEs in the residues in βB involved in the peptide-binding interaction were found to change dramatically upon peptide binding (Fig. 4A and B). Most of the residues in αA, αB, βA, βB, βD, and βE showed high XNOE values in the absence of DBM peptide. However, residues located at the portal of the peptide-binding pocket (at the beginning of βB and βC) had lower XNOEs, indicating the flexibility of the protein. B-factors of Dvl1 PDZ in the crystal structure suggest that PDZ domain is relatively rigid in most of the secondary structural regions (shown in green color in Fig. 4C). However, a loop between βA and βB, and αB, which are involved in peptide binding, showed higher values (shown in red color in Fig. 4C), showing that this region is dynamic (Fig. 4C). Our data provide detailed information about the Dvl1/CXXC5 interaction and the dynamic profile of Dvl PDZ, which will be useful for designing an inhibitor of Dvl1.

Acknowledgements

This work was supported by the National Research Foundation of Korea (NRF) through their Mid-career Researcher Program (grant number NRF-2013R1A2A2A01068963) and the Translational Research Center for Protein Function Control (grant number 2016R1A5A1004694).

Transparency document

Transparency document related to this article can be found online at http://dx.doi.org/10.1016/j.bbrc.2016.12.023.

References

[1] R.T. Moon, A.D. Kohn, G.V.D. Ferrari, A. Kaykas, WNT and beta-catenin signalling: diseases and therapies, Nat. Rev. Genet. 5 (2004) 691–701.
[2] R. Nusse, Wnt signaling in disease and in development, Cell Res. 15 (2005) 28–32.
[3] C.Y. Logan, R. Nusse, The Wnt signaling pathway in development and disease, Annu. Rev. Cell. Dev. Biol. 20 (2004) 781–810.
[4] A. Klaus, W. Birchmeier, Wnt signalling and its impact on development and cancer, Nat. Rev. Cancer 8 (2008) 387–398.
[5] J.B. Wallingford, R. Habas, The developmental biology of Dishevelled: an enigmatic protein governing cell fate and cell polarity, Development 132 (2005) 4421–4436.
[6] Y. Komiya, R. Habas, Wnt signal transduction pathways, Organogenesis 4 (2008) 68–75.
[7] W. Pan, S.C. Choi, H. Wang, Y. Qin, L. Volpicelli-Daley, L. Swan, L. Lucast, C. Khoo, X. Zhang, L. Li, C.S. Abrams, S.Y. Sokol, D. Wu, Wnt3a-mediated formation of phosphatidylinositol 4,5-bisphosphate regulates LRP6 phosphorylation, Science 321 (2008) 1350–1353.
[8] H.C. Wong, J. Mao, J.T. Nguyen, S. Srinivas, W. Zhang, B. Liu, L. Li, D. Wu, J. Zheng, Structural basis of the recognition of the dishevelled DEP domain in the Wnt signaling pathway, Nat. Struct. Biol. 7 (2000) 1178–1184.
[9] C. Gao, Y.G. Chen, Dishevelled: the hub of Wnt signaling, Cell. Signal. 22 (2010) 717–727.
[10] H.C. Wong, A. Bourdelas, A. Krauss, H.J. Lee, Y. Shao, D. Wu, M. Mlodzik, D.L. Shi, J. Zheng, Direct binding of the PDZ domain of Dishevelled to a conserved internal sequence in the C-terminal region of Frizzled, Mol. Cell 12 (2003) 1251–1260.
[11] C. Punchihewa, A.M. Ferreira, R. Cassell, P. Rodrigues, N. Fujii, Sequence requirement and subtype specificity in the high-affinity interaction between human frizzled and dishevelled proteins, Protein Sci. 18 (2009) 994–1002.
[12] N. Barker, H. Clevers, Mining the Wnt pathway for cancer therapeutics, Nat. Rev. Drug Discov. 5 (2006) 997–1014.
[13] T. Andersson, E. Södersten, J.K. Duckworth, A. Cascante, N. Fritz, P. Sacchetti, I. Cervenka, V. Bryja, O. Hermanson, CXXC5 is a novel BMP4-regulated modulator of Wnt signaling in neural stem cells, J. Biol. Chem. 284 (2009) 3672–3681.
[14] H.Y. Kim, J.Y. Yoon, J.H. Yun, K.W. Cho, Y.M. Rhee, H.S. Jung, H.J. Lim, J. Choi, J.N. Heo, W. Lee, K.T. No, D. Min, K.Y. Choi, CXXC5 is a negative-feedback regulator of the Wnt/β-catenin pathway involved in osteoblast differentiation, Cell Death Differ. 22 (2015) 912–920.
[15] H.J. Lee, N.X. Wang, D.L. Shi, J. Zheng, Sulindac inhibits canonical Wnt signaling by blocking the PDZ domain of the protein Dishevelled, Angew. Chem. Int. Ed. 48 (2009) 6448–6452.
[16] Z. Otwinowski, W. Minor, Processing of X-ray diffraction data collected in oscillation mode, Meth. Enzymol. 276 (1997) 307–326.
[17] P.D. Adams, P.V. Afonine, G. Bunkóczi, V.B. Chen, I.W. Davis, N. Echols, J.J. Headd, L.W. Hung, G.J. Kapral, R.W. Grosse-Kunstleve, A.J. McCoy, N.W. Moriarty, R. Oeffner, R.J. Read, D.C. Richardson, J.S. Richardson, T.C. Terwilliger, P.H. Zwart, PHENIX: a comprehensive Python-based system for macromolecular structure solution, Acta Cryst. D 66 (2010) 213–221.
[18] P. Emsley, K. Cowtan, Coot: model-building tools for molecular graphics, Acta Cryst. D 60 (2004) 2126–2132.
[19] A. Vagin, A. Teplyakov, MOLREP: an automated program for molecular replacement, J. Appl. Cryst. 30 (1997) 1022–1025.
[20] N. London, B. Raveh, E. Cohen, G. Fathi, O. Schueler-Furman, Rosetta FlexPepDock web server–high resolution modeling of peptide-protein interactions, Nucleic Acids Res. 39 (2011) W249–W253.
[21] B. Raveh, N. London, O. Schueler-Furman, Sub-angstrom modeling of complexes between flexible peptides and globular proteins, Proteins 78 (2010) 2029–2040.
[22] R. Das, D. Baker, Macromolecular modeling with rosetta, Annu. Rev. Biochem. 77 (2008) 363–382.
[23] G.W. Vuister, A. Bax, J. Am. Chem. Soc. 115 (1993) 7772–7777.
[24] A. Grzesiek, A. Bax, J. Magn. Reson B102 (1993) 103–106.
[25] D. Cowburn, Peptide recognition by PTB and PDZ domains, Curr. Opin. Struct. Biol. 7 (1997) 835–838.
[26] Y. Ivarsson, Plasticity of PDZ domains in ligand recognition and signaling, FEBS Lett. 17 (2012) 2638–2647.
[27] J.H. Lee, H. Park, S.J. Park, H.J. Kim, S.H. Eom, The structural flexibility of the shank1 PDZ domain is important for its binding to different ligands, Biochem. Biophys. Res. Commun. 407 (2011) 207–212.